Ceramics International 46 (2020) 24379–24384

Contents lists available at ScienceDirect

Ceramics International

journal homepage: www.elsevier.com/locate/ceramint

Effects of exposure time and printing angle on the curing characteristics and flexural strength of ceramic samples fabricated via digital light processing

Minhao Shen[a,1], Weiming Zhao[a,1], Bohang Xing[b], Ying Sing[a], Shuyue Gao[a], Cao Wang[a,**], Zhe Zhao[a,c,*]

[a] School of Materials Science and Engineering, Shanghai Institute of Technology, Shanghai, 201418, China
[b] School of Material Science and Engineering, Tianjin University, NW, Tianjin, 300072, China
[c] Department of Materials Science and Engineering, KTH Royal Institute of Technology, Stockholm, SE-100 44, Sweden

ARTICLE INFO

Keywords:
Exposure time
Print angle
DLP
Zirconia

ABSTRACT

The development of photosensitive slurries for additive manufacturing has attracted great interest due to their correlation with the final properties of the fabricated parts. This paper focus on the printing quality control in digital light processing (DLP) 3D printing of advanced ceramics. Systematic experiments were performed to assess the effects of the exposure time and printing angle on the three-point bending strength of the fabricated samples. The exposure time affected the bending strength of the printed zirconia ceramic dramatically. When the weak exposure time is 1 s and the strong exposure time is 13 s, the average bending strength can reach 580 MPa while Weibull modulus can reach 8.84. Meanwhile, the printing angle also affected the bending strength mechanical sample printed at 45° exhibits the worst performance.

1. Introduction

Ceramic components are usually utilized in traditional techniques, such as injection moulding, dry pressing, and moulding. To achieve densification, these materials need to be sintered at high temperature. However, these fabrication techniques limit the development of ceramics due to their low efficiency and high consumption. The emergence of 3D printing technology provides a possibility to solve the difficulty in ceramic preparation and forming. Ceramic UV-curing 3D printing is a manufacturing technology that utilizes digital light processing (DLP) to fabricate ceramic features [1–3]. Ceramic 3D printing is a customizable process that can produce nearly any geometry without the use of expensive moulds and tooling; accordingly, this fabrication approach can be applied for many applications in the field of engineering technology, such as in ceramic implants [4], biomedical scaffolds [5], and heat exchangers [6].

DLP is a mask-based stereolithography in which an integral image is transferred to a photopolymerizable liquid surface by exposing the light source through a patterned mask only once [7].

The stable and homogeneous suspension used for this process consists of a photosensitive resin monomer, a photoinitiator, a light absorber, a dispersant and zirconia particles. To obtain dense sintered samples without defects and cracks, the solid loading of the ceramic suspension must be higher than 40 vol% [8]. For a given slurry, the curing depth increases with increasing exposure time until a certain limit. However, exceeding this limit will overexpose the sample, causing it to curl and arch [9,10]. Actually, the properties of the fabricated samples also depend on the exposure mode. A previous study revealed that there were five exposure modes: pulse, ramp, soft-start, pulse delay and constant exposure [11]. The results of this study showed that these exposure modes helped decrease the polymerization shrinkage stress. Nicoleta Ilie et al. [12] studied the influence of soft-start exposure on shrinkage stress, curing degree and mechanical properties. Their results showed that although the curing degree was reduced by 10%, the mechanical properties remained unchanged, and the shrinkage stress was reduced. But all these investigation with various exposure modes focused on the curing behavior of thick layers or bulk materials. Wu [13] et al.'s results showed that the soft-start exposure mode was beneficial both to reduce size errors caused by light scattering and to improve mechanical properties of high purity alumina. But the relatively poor strength and limited samples for Weibull modulus study made the conclusion not very convincing. Mario Borlaf et al. [14] showed a reasonably good bending strength and Weibull modulus based on their careful selection with the exposure time. It

* Corresponding author. School of Materials Science and Engineering, Shanghai Institute of Technology, Shanghai, 201418, China.
** Corresponding author.
E-mail addresses: wangcaocc@gmail.com (C. Wang), zhezhao@kth.se (Z. Zhao).
[1] These authors contributed equally to this work and should be considered co-first authors.

https://doi.org/10.1016/j.ceramint.2020.06.220
Received 13 February 2020; Received in revised form 18 June 2020; Accepted 19 June 2020
Available online 20 June 2020
0272-8842/ © 2020 Elsevier Ltd and Techna Group S.r.l. All rights reserved.

seems that the soft-start exposure might be not really necessary for excellent mechanical properties. So far, the highest bending strength of 1154 MPa of 3Y-TZP ceramic was reported by Xing et al. [15] with very limited data showing how the printing parameters will affect the final mechanical properties. Unfortunately, the tremendous fracture wrinkles and tiny triple-joint boundary pores suggested that the reported mechanical property may contain some technical errors. An grain boundaries had better mechanical properties. Similarly, Reham B. Osman et al. [4] got relatively high bending strength of ~1000 MPa based on a biaxial flexure test, which in general will give a higher value than 3-point or 4-point bending test. Very interesting, they also demonstrated that the printing angle doesn't influence the strength dramatically. This also indicate that except for the exposure time and mode, there might be other factors can be more decisive for the mechanical properties of the 3D-printed ceramics. We also noticed that both Mario Borlaf et al. [14] and Reham B. Osman et al. [4] used a layer thickness much less than 50 μm, which is more preferred for a better production efficiency.

In this study, we aim to understand if a normal exposure mode with appropriate exposure time can be possible for improved mechanical property when a reasonable printing thickness of 50 μm was remained to keep the production efficiency acceptable for potential industry interest. To evaluate the effect of proper exposure time selection, we also implemented study on the effect of printing orientation on the final mechanical strength.

2. Experimental process

2.1. Material and fabrication processing

A 3 mol% yttrium-stabilized zirconia (3Y-TZP) suspension with a solid load of 50 vol% and a top-down DLP printer were both provided by Jiaxing CeramPlus Tech. Co. LTD. (Zhejiang Province, China). The slurry showed a typical shear-thinning behaviour and can be stored in a light-shield black plastic bottle at room temperature for three months without noticeable sedimentation. The x-y plane resolution of the DLP printer was 50 μm. The wavelength of the UV light was 405 nm, and the printing layer thickness was set as 50 μm. The printing process was carried out at room temperature. After the printing process, the extra slurry was cleaned off the sample surface with ethanol, and then a secondary 30 s UV curing was implemented.

To investigate the influence of different exposure times on the strength of printed zirconia ceramics, the time of weak exposure was kept as 1 s (this is actually one bug for the software, it is necessary to keep this value not to be zero), and the normal exposure time was set at 2 s, 3 s, 4 s, 5 s, … 14 s. To make our result to be comparable to other DLP printing research, we set the normal irradiation intensity to be 8.5mw/cm^2 and the intensity was reduced to be half of the normal intensity by default. For each exposure time, 10 bending bar samples with geometry size of 35 × 4x3mm were printed, sintered and tested for 3-point bending strength. For each printing angle, 50 bending bars were prepared at exposure time of 13s and tested for 3-pinting bending strength. To evaluate the reliability of the studied DLP-printing technique, we also calculated Weibull modulus for all the above-mentioned strength test. It is worth noting that the printing angle was changed along the X-axis (see Fig. 8).

To avoid damage in the transfer process, a one-step sintering method was adopted, which means that only one traditional muffle furnace (KF1700, Nanjing Boyuntong Instrument Technology Co., Ltd., China) was used in the debinding and sintering process. It is critical that all specimens should be sintered as soon as possible after their fabrication to eliminate possible effects of environmental conditions on the mechanical properties of the ceramics. The sintering profile was described in detail in the results and discussion section.

2.2. Flexural strength tests of the sintered bars

The dimensions of the specimens were 35 mm × 4 mm × 3 mm (length, width, thickness), and the size of the final sintered samples slightly deviated from the set value due to light scattering and resolution accuracy of the printer; however, the observed error was acceptable. The mechanical behaviour of ceramics is strongly dependent on the applied strain rate, material type, and sintering schedule. The three-point bending tests were performed in accordance with ISO 14704:2000 on a universal testing machine (SUN500, Cardanoal Camp, Italy). The loading direction was parallel to the DLP building direction. The maximum load required to fracture the specimen was recorded. Prior to testing, the samples were visually inspected to exclude artificial defects, the support structures were removed and no further surface finishing was implemented after printing and cleaning.

2.3. Characterization

The thermal decomposition of the resin was analysed by thermogravimetric analysis (TGA) in air between 20 and 650 °C using a heating rate of 1 °C/min. The density of the sintered samples was measured by the Archimedes method (sartorius, Germany). The flexural strength of the sintered sample was determined on a three-point bending tester (SUN500, Cardanoal Camp, Italy) with a span of 30 mm and a loading rate of 0.5 mm/min. The fracture surface microstructure of the sintered samples was examined with a scanning electronic microscope (Phenom Pro, Phenom World, Netherlands).

3. Results and discussion

Fig. 1 shows the TG (thermogravimetry)-DSC curves of the green body obtained after printing with the ceramic UV resin. To obtain a dense ceramic sample, we need to carry out a debinding process to remove organic matter from the green body [16]. The cured resin began to decompose after 150 °C, it is mainly water evaporation before this temperature. The thermal decomposition finished before 500 °C. There are three main decomposition peaks around 180 °C, 330 °C and 450 °C. The resin decomposed quickly between 180 °C and 350 °C during the debinding process. To avoid the rapidly expanding gas exacerbating the defects in the low-temperature debinding stage [17], the temperature rise rate between 100 and 500 °C should be carefully controlled.

Fig. 2 shows the temperature profile for the debinding and sintering process. The following debinding and sintering profiles were used: various heating rate of 2 °C/min, 0.5 °C/min, 0.25 °C/min and 1 °C/min

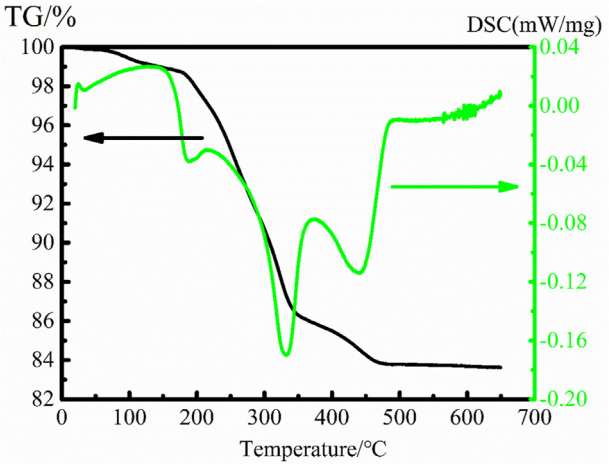

Fig. 1. TGA results for zirconia: weight (black line) and differential scanning calorimetry (DSC, green line). (For interpretation of the references to colour in this figure legend, the reader is referred to the Web version of this article.)

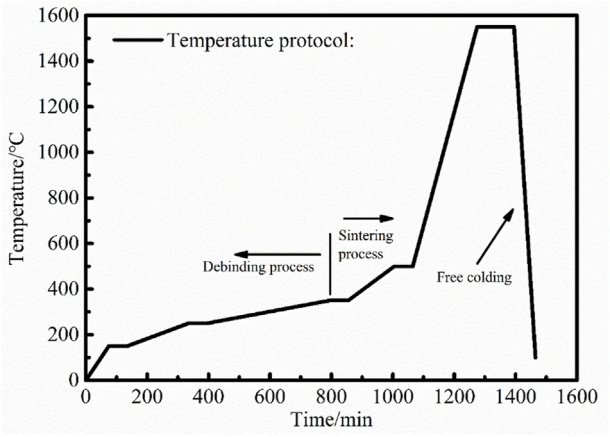

Fig. 2. Debinding and sintering temperature profile.

were implemented for the temperature range of RT-150 °C, 150–250 °C, 250–350 °C and 350–500 °C. Meanwhile we applied 60min for dwelling at temperatures of 150 °C, 250 °C, 350 °C and 500 °C to let the chemical reaction got finished. After debinding process up to 500 °C, a heating rate of 5 °C/min was applied for the whole sintering up to 1550 °C and hold for 120min.

Fig. 3 shows that the sintered zirconia ceramic possesses a dense and uniform microstructure with a grain size of approximately 1 μm. After sintering at 1550 °C, the density of the 3Y-TZP ceramic was ≥6.01 g/cm^3, which is approximately 99% relative density if 6.07 g/cm^3 was taken as the theoretical density. Potentially, we can expect that the mechanical properties of the studied bars got limited influence from the microstructural defects. The obtained mechanical properties can be regarded as the direct reflection of the printing quality or the macrostructural defects linked with the printing lamination and polymerization process.

In DLP, the curing thickness is an important parameter that determines the usable layer thickness and printing quality. It is essential to find proper exposure time to guarantee good bonding between the cured layers during the printing process. Therefore, the curing depth under different exposure times was tested with a special computer-aided-design (CAD) model (see the illustration in Fig. 4(a)). The hollow part of the model is cured for only one layer with a series of exposure time increased from the left to the right, starting from 1s. The results are shown in Fig. 4(a), and it can be found that as the exposure time increases, the curing depth also increases. The minimum curing depth is about 30 μm. When the exposure time is greater than 11 s, the curing depth is not changing anymore and it is always about 120 μm.

To determine the penetration depth and critical exposure energy of the ceramic slurry, the Beer-Lambert law, which expresses the absorption and attenuation characteristics of light propagation in different media, has been utilized. This law is expressed as follows:

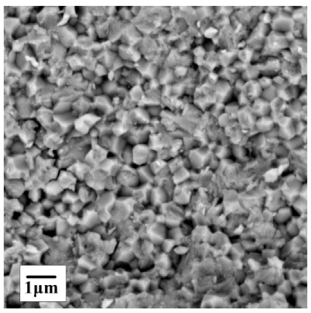

Fig. 3. SEM image of the fracture surface of the sintered ZrO2 ceramic (exposure time of 13s).

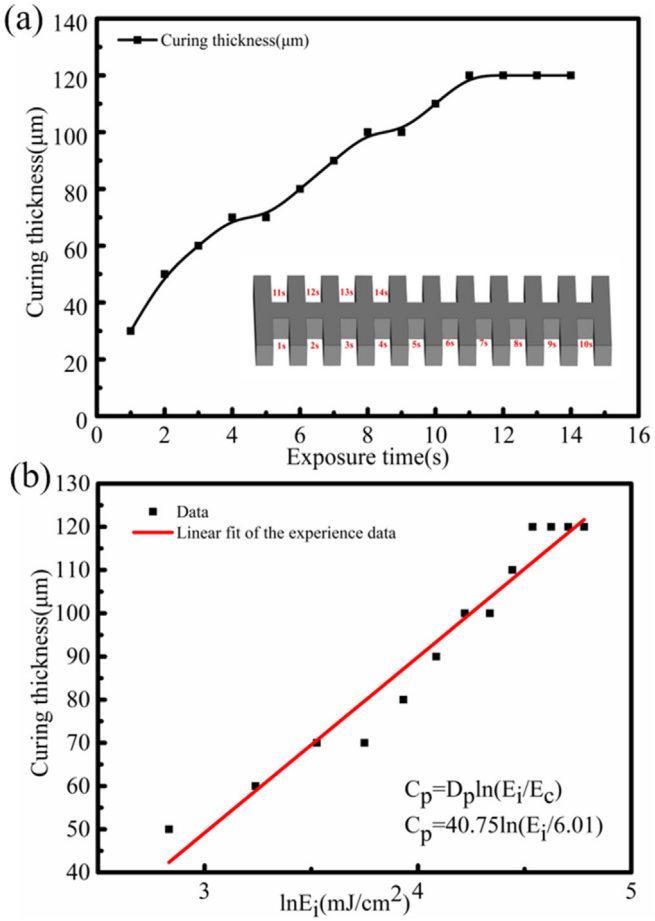

Fig. 4. (a) Curing depth under different exposure times for curing characteristics tests; the inset shows the test part geometry used for the cure-depth analysis. (b) Beer-Lambert law fitting.

$$C_p = D_p \ln\left(\frac{E_i}{E_C}\right) = D_p \ln E_i - D_p \ln E_c \tag{1}$$

where C_p is the curing thickness, D_p is the penetration depth, and E_c is the critical exposure energy of the ceramic slurry. When the light intensity is less than the critical exposure energy, the slurry will not be cured. Both D_p and E_c depend on the properties of the ceramic slurry. E_i is the energy input to the UV resin ceramic slurry, which is determined by the exposure parameters of the DLP light source.

$$E_i = W_i \times t \tag{2}$$

where W_i (mW/cm^2) is the exposure intensity and t (s) is the exposure time. According to the parameters provided by the manufacturer, the total effective light intensity (W_i) of the light engine is measured to be 8.5 mW/cm^2.

After measuring the curing thickness, the logarithmic value of the exposure energy was taken as the abscissa value and the thickness value was taken as the ordinate value to get data fitted with equation (1). The point series were fitted with a straight line. The slope of the line was D_p, and the intersection of the line with the X-axis was E_c. Fig. 4(b) shows the linear fit results, and it can be found that D_p is 40.75 μm while E_c is 6.01 (mJ/cm^2). The following fitting equation can be used to predict the curing thickness with the exposure time/energy.

$$C_p = 40.75 \ln\left(\frac{E_i}{6.01}\right) \tag{3}$$

In general, with the increase of exposure energy (E_i), the curing thickness (C_p) also gradually increased. But in reality we can find that there is no increase in curing thickness after a exposure time of 11s.

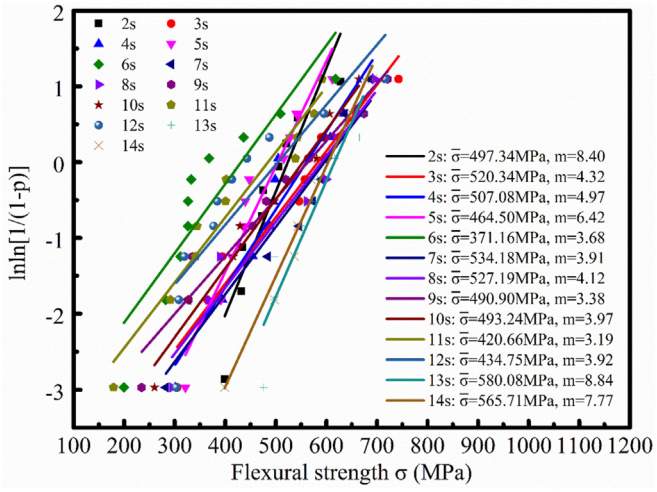

Fig. 5. Flexural strength data and the corresponding Weibull moduli of the sintered bending samples fabricated under different exposure times ($\bar{\sigma}$ is the average flexural strength and m is the Weibull moduli).

Thus we would like to conclude that this Beer-Lmbert law can only predict the curing behavior with limited availability. The continuous change in the transmittance of the cured ceramic resin layer should be the key reason for such a behavior. It was essential to do a real test for each new slurry to get proper printing parameters.

Fig. 5 shows the three-point bending strength of test bars fabricated under different exposure times and calculates their Weibull moduli [18]. The reliability of ceramic materials is represented by the Weibull modulus (named m), which characterizes the defect distribution in the specimen and the statistic variation in the population of defects among the tested samples. In general, a lower Weibull modulus indicates a worse material quality and processing reliability.

Fig. 5 shows that the bars with a 13 s exposure time has a flexural strength of 580 MPa and a Weibull modulus of 8.84, which are both the highest values observed among the tested samples. The flexural strength of samples fabricated with a similar preparation technique in the literature ranges from 561 to 878 MPa [19,20], which fits with the results of this paper. It is undeniable that there is still a certain gap between the results in this study and the highest levels achieved in the literature.

The flexural strength of the samples under other exposure conditions was lower than 561 MPa, the worst of which was the sample with an exposure time of 6 s, for which the flexural strength was only 371 MPa and the Weibull modulus was 3.68. Fig. 4(b) shows that the D_p of the ceramic suspensions was 40 μm. When the exposure time was 13 s, the curing depth was 120 μm, which is three times the value of D_p; the highest bending strength was obtained under these conditions. When the exposure time was 6 s, the curing depth was 80 μm, which is twice the value of D_p; the lowest flexural strength was obtained under this condition.

To further understand the reason behind this change in bending strength with the exposure time, we investigated the fracture mode and also the microstructure of the bending bars. In Fig. 6, it was clear that 13s exposure time led to a rather sharp and even fracture surface and 6s exposure time led to a uneven fracture mode with indication of weak defects along the interlayer boundaries direction. For sure that the interlayer bonding directly decide the final bending strength and Weibull modulus. A proper exposure time seems to be very critical for the printing quality control. Further study with the SEM analysis (see Fig. 7) can also provide extra evidence for the interlayer bonding conditions. Even though only free surface were selected in this study, clear lamination were quite obvious at lower magnification. Noticeable difference can be found at higher magnification for the sites along the

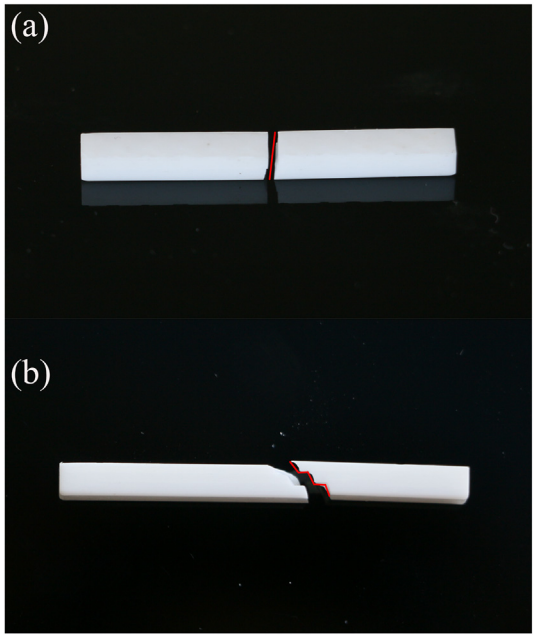

Fig. 6. Images of the freshly fractured bending bars: (a) 13s exposure time and (b) 6s exposure time.

interlayer boundaries. The interlayer boundary area for the 13s exposure time sample is smooth and dense, no clear boundary or defects (pores) can be easily identified, while a lot of loosely distributed pores can be seen along the interlayer boundary for the 6s exposure time sample. It is rational to expect that a better interlayer bonding with less pores can promise a high bending strength [10]. Both fracture mode and local microstructural analysis demonstrate that the key reason for the change of mechanical property is the change of the interlayer bonding strength. Better interlayer bonding also lead to higher Weibull modulus.

For this study, it is more interesting that the interlayer bonding condition didn't follow the curing depth linearly. Clearly, there is a bottom around 6s between two peaks of 3s and 13s exposure time if we use the final bending strength to judge the effect of the exposure time on the printing quality. As we already saw the steady increase of curing depth with the exposure time up to 12s (see Fig. 4(a)), it is clear that the increased curing depth didn't solely decide the binding strength between adjacent layers. The thermal stress generated during the polymerization of UV resin had been widely accepted being one factor influence the final property of the cured UV resin. Out result should be also one reflection of the complex thermal stress condition during the curing process. In Li et al. ‘s [21] study, they demonstrated that the secondary conversion of ceramic UV resin in multiple layers was possible. The transmitted light could effectively induce further polymerization in the cured layers. The existence of a conversion rate increase in the cured layer caused by a decayed incident light was proven by changes in temperature over the extended curing process. There is a certain incident energy and layer thickness to promise a higher monomer to polymer conversion rate and thus a good chemical bonding between layers. Thus, we tentatively conclude that the best mechanical properties obtained at 13s exposure time should be the result of this secondary conversion behaviour. The relatively good mechanical properties for the 3s exposure time should be the indication of the primary conversion mentioned in Li et al.'s [21]study. As the exposure time extended over 3s, there is still a continuous polymerization in the cured layer which was initiated by the decayed light irradiation, thus the extended light irradiation might lead to local temperature rise or local polymerization which may introduce local stress or defects. Till the time cured layer also underwent a full secondary conversion, the

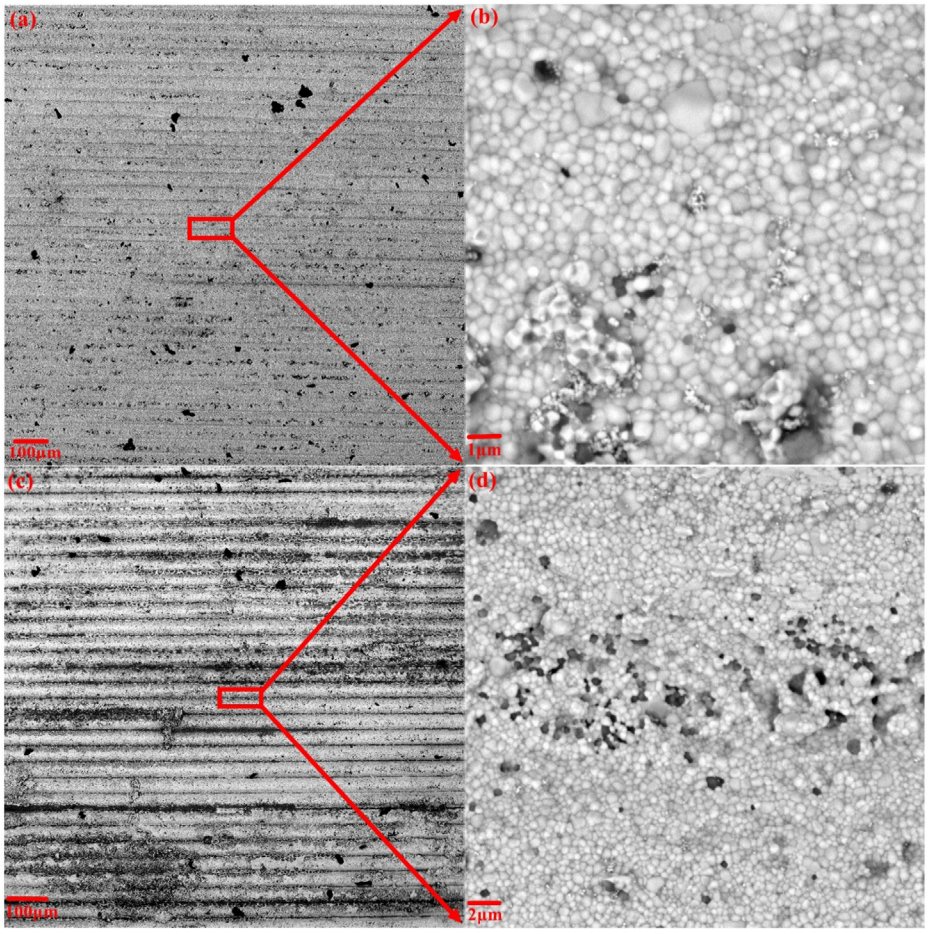

Fig. 7. Fracture microstructure of the ceramic bars with different three-point bending strengths: (a, b) the bar with the highest flexural strength and (c, d) and the bar had the lowest flexural strength.

binding strength between layers can be expected. Very interestingly, a very similar primary and secondary conversion exposure time (3 and 12s) was found in a Al_2O_3 ceramic UV resin slurry.

Fig. 8 shows CAD models of test bars with different printing angles. The 0° and 90° printer specimens do not need support, whereas the other bars need support structure, which is not shown in the figure. The angle shown in the figure is the angle of rotation along the X-axis. The pressure direction of the test sample is perpendicular to the surface, which has dimensions of 3 mm × 4 mm × 35 mm, regardless of how the printing direction is changed.

Fig. 9 shows the flexural strength data and corresponding Weibull modulus calculations of the sintered bending samples fabricated under different printing angles. When the number of samples increased from 10 to 50, we can see that the three-point bending strength and Weibull modulus of the 0° printing bars got decreased, compared with the results presented in earlier part of this study. The greater the number of samples is, the better the tests can reflect the real situation. Obviously, there is still room for improvement in the technical stability of DLP. It is interesting that when the rotation angle is close to 45°, the flexural strength decreases, and vice versa. The sample printed at 45° has the worst flexural strength and reliability, which is in agreement with Reham B. Osman et al.'s [4] results. This behaviour may be attributed to the difficulty in attaching subsequent layers to the shape fabricated with a 45° build angle, which results in more structural defects in the printed object. Note that 15° and 75° and 30° and 60° are symmetric

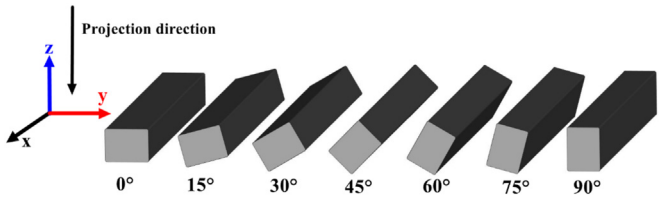

Fig. 8. CAD model of test bars with different printing angles.

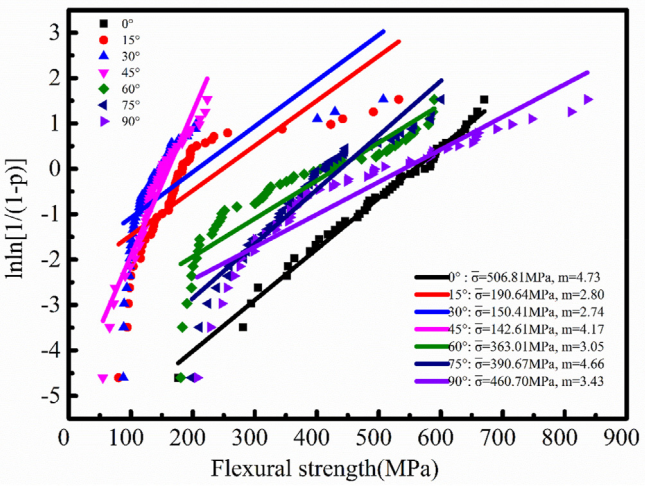

Fig. 9. Flexural strength data and the corresponding Weibull moduli of the sintered bending samples fabricated under different printing angles ($\bar{\sigma}$ is the average flexural strength and m is the Weibull moduli).

about the Z-axis, and the flexural strength and printing stability of the test bars prepared at 60° and 75° were better than those prepared at 30° and 15°. This finding shows that 3D printing has a certain directivity rather than complete isotropy, and the direction needs to be considered in the printing process. The number of samples in the literature [22] was 30, the measured three-point bending strength was 300 MPa–580 MPa, and the Weibull modulus was 11.2. Compared with the measured data, we increased the number of samples to 50, the Weibull modulus decreased considerably, and the printing stability decreased. At printing angles of 15°, 30° and 45°, the strength of the sample was lower than 300 MPa, and the strength of the sample prepared at printing angles of 60°, 75° and 90° was within the range in the literature. The printing quality changed with the printing angle, this fact also indicate that the optimized exposure time obtained from the first part of this study didn't resolve all the interlayer bonding problems even though a relatively good result can be obtained.

Similar to other 3D printing technologies, there are still some problems in the lamination process and sintering process of printing parts with DLP preparation technology [23]. Without considering the post-processing and debinding process (organic matter turns into gas at high temperature) of green bodies, the binding strength between layers is the key bottle-lock problem for the future industry application. We can expect that more detailed study with the curing process itself is necessary for the future development. It can for sure to expect that the 3D printed ceramic materials can be comparable to other advanced ceramic processing techniques in aspect of properties, if light-materials interaction can be understood better.

4. Conclusion

This work investigated the influences of exposure time and printing angle on the DLP manufacturing technique. When the exposure time was 3s and 13 s, the three-point bending strength reached 520 and 580 MPa respectively. While the 13s led to a doubled Weibull modulus. Even the curing depth increased with increasing exposure time, the increase in curing depth did not necessarily promise better mechanical properties. The complex curing behaviour in the freshly cured and cured layers was believed to be the key reason for the demonstrated wave-like change in strength over the exposure time. The flexural strength of the sample was the worst at a printing angle of 45°. This finding indicates that 3D printing is anisotropic, and the printing angle should be taken into account during sample fabrication. To obtain printed parts with high strength, there is still a need to understand the curing process in a better manner to get DLP-printed ceramics to be applicable for industry mass-production.

Declaration of competing interest

The authors declare that they have no known competing financial interests or personal relationships that could have appeared to influence the work reported in this paper.

Acknowledgements

The authors gratefully acknowledge the financial support provided by the National Key R&D Program of China (No. 2017YFB1103500 & No. 2017YFB1103502). The findings, conclusions, and recommendations expressed in this manuscript are those of the authors and do not necessarily reflect the views of the NKPC.

References

[1] T. Chartier Cc, F. Doreau, M. Loiseau, Stereolithography of structural complex ceramic parts, J. Mater. Sci. 37 (2002) 3141–3147.
[2] Tassilo Moritz, Saeed Maleksaeedi, Additive manufacturing of ceramic components, in: Zhang Jing, Yeon-Gil Jung (Eds.), Additive Manufacturing, butterwort-Heinemann, 2018.
[3] J. Zhang, L. Wei, X. Meng, F. Yu, N. Yang, S. Liu, Digital light processing-stereolithography three-dimensional printing of yttria-stabilized zirconia, Ceram. Int. 46 (2020) 8745–8753.
[4] R.B. Osman, A.J. van der Veen, D. Huiberts, D. Wismeijer, N. Alharbi, 3D-printing zirconia implants; a dream or a reality? An in-vitro study evaluating the dimensional accuracy, surface topography and mechanical properties of printed zirconia implant and discs, J. Mech. Behav. Biomed. Mater. 75 (2017) 521–528.
[5] E. Schwarzer, S. Holtzhausen, U. Scheithauer, C. Ortmann, T. Oberbach, T. Moritz, et al., Process development for additive manufacturing of functionally graded alumina toughened zirconia components intended for medical implant application, J. Eur. Ceram. Soc. 39 (2019) 522–530.
[6] U. Scheithauer, E. Schwarzer, T. Moritz, A. Michaelis, Additive manufacturing of ceramic heat exchanger: opportunities and limits of the lithography-based ceramic manufacturing (LCM), J. Mater. Eng. Perform. 27 (2017) 14–20.
[7] Z. Chen, Z. Li, J. Li, C. Liu, C. Lao, Y. Fu, et al., 3D printing of ceramics: a review, J. Eur. Ceram. Soc. 39 (2019) 661–687.
[8] L. Michelle, J.W.H. Griffith, Freeform fabrication of ceramics via stereolithography, J. Am. Ceram. Soc. 79 (1996) 2601–2608.
[9] M. Dewaele, E. Asmussen, A. Peutzfeldt, E.C. Munksgaard, A.R. Benetti, G. Finne, et al., Influence of curing protocol on selected properties of light-curing polymers: degree of conversion, volume contraction, elastic modulus, and glass transition temperature, Dent. Mater. 25 (2009) 1576–1584 official publication of the Academy of Dental Materials.
[10] G. Mitteramskogler, R. Gmeiner, R. Felzmann, S. Gruber, C. Hofstetter, J. Stampfl, et al., Light curing strategies for lithography-based additive manufacturing of customized ceramics, Add. Manuf. 1–4 (2014) 110–118.
[11] E.A. Munchow, C.T.W. Meereis, W.L. de Oliveira da Rosa, A.F. da Silva, E. Piva, Polymerization shrinkage stress of resin-based dental materials: a systematic review and meta-analyses of technique protocol and photo-activation strategies, J. Mech. Behav. Biomed. Mater. 82 (2018) 77–86.
[12] N. Ilie, E. Jelen, R. Hickel, Is the soft-start polymerisation concept still relevant for modern curing units? Clin. Oral Invest. 15 (2011) 21–29.
[13] X. Wu, Q. Lian, D. Li, X. He, X. Liu, J. Meng, et al., Effects of soft-start exposure on the curing characteristics and flexural strength in ceramic projection stereolithography process, J. Eur. Ceram. Soc. 39 (2019) 3788–3796.
[14] M. Borlaf, A. Serra-Capdevila, C. Colominas, T. Graule, Development of UV-curable ZrO2 slurries for additive manufacturing (LCM-DLP) technology, J. Eur. Ceram. Soc. 39 (2019) 3797–3803.
[15] H. Xing, B. Zou, S. Li, X. Fu, Study on surface quality, precision and mechanical properties of 3D printed ZrO2 ceramic components by laser scanning stereolithography, Ceram. Int. 43 (2017) 16340–16347.
[16] K. Zhang, R. He, G. Ding, C. Feng, M. Xia, W. Song, et al., Digital light processing of 3Y-TZP strengthened ZrO2 ceramics, Mater. Sci. Eng., A (2019) 138768.
[17] K. Wang, M. Qiu, C. Jiao, J. Gu, D. Xie, C. Wang, et al., Study on defect-free debinding green body of ceramic formed by DLP technology, Ceram. Int. 46 (2020) 2438–2446.
[18] W. weibull, A statistical distribution function of wide applicability, J. Appl. Mech. 18 (1951) 293–297.
[19] W. Harrer, M. Schwentenwein, T. Lube, R. Danzer, Fractography of zirconia-specimens made using additive manufacturing (LCM) technology, J. Eur. Ceram. Soc. 37 (2017) 4331–4338.
[20] J.-C. Wang, H. Dommati, Fabrication of zirconia ceramic parts by using solvent-based slurry stereolithography and sintering, Int. J. Adv. Manuf. Technol. 98 (2018) 1537–1546.
[21] X. Li, K. Hu, Z. Lu, Effect of light attenuation on polymerization of ceramic suspensions for stereolithography, J. Eur. Ceram. Soc. 39 (2019) 2503–2509.
[22] M. Schwentenwein, J. Homa, Additive manufacturing of dense alumina ceramics, Int. J. Appl. Ceram. Technol. 12 (2015) 1–7.
[23] W. Oropallo, L.A. Piegl, Ten challenges in 3D printing, Eng. Comput. 32 (2015) 135–148.